

## Localized short impulses in a nerve model with self-excitable membrane

Alain M. Dikandé\* and Ga-Akeku Bartholomew

Laboratory of Research on Advanced Materials and Nonlinear Sciences (LaRAMaNS), Department of Physics, Faculty of Science,  
University of Buea, P.O. Box 63, Buea, Cameroon

(Received 26 May 2009; revised manuscript received 22 July 2009; published 5 October 2009)

During the generation and transmission of nerve impulses, the cytoplasm behaves like an excitable medium that self-regulates the shapes and magnitudes of the output excitation. In connection with this self-regulatory function, one can readily think of the plasma membrane as a nerve organ holding the key role in the mechanisms of generation and transmission of the transmembrane potential, namely, it is expected to provide the essential feedback that stabilizes the stimulus. Here, a simple and coherent picture of self-regulation of the nerve impulse is proposed in terms of one single feedback associated with the main excitable biological organ of the nervous system. In this purpose, an electrodynamic theory is developed within the framework of a cable model in which the membrane capacitor is regarded as a charge-management electrical component with a defined capacity-voltage characteristic. It is found that in both myelinated and myelin-free nerve fiber contexts, the transmembrane excitations are well-localized short impulses whose shape and stability are determined by the capacity-voltage characteristic assumed to govern the self-excitability properties of the nerve membrane.

DOI: [10.1103/PhysRevE.80.041904](https://doi.org/10.1103/PhysRevE.80.041904)

PACS number(s): 87.10.Ed

### I. INTRODUCTION

The nerve conduction represents one of the most investigated physiological activities from both experimental and theoretical standpoints, and currently a wealth of electrophysiological recordings is available on this activity in connection with several families of biological systems including humans and animals. According to these electrophysiological data the nerve impulse is a self-regenerative pulse wave associated with the electrochemical activity of biological organs, the main function of which is to allow excitable cells such as muscle and nerve cells to carry a signal over a long distance [1,2] throughout the nervous system. It is a propagating form of the primary electrical signal generated by nerve cells, the so-called action potential [3,4] arising from changes in the permeability of the nerve cell's axonal membranes to specific ions.

As now well established, during the generation and transmission of the nerve impulse [3–8], the leading edge of the depolarization region triggers adjacent membranes to depolarize causing a self-propagation of the excitation related to the transmembrane potential down the nerve fiber [9]. As first suggested by Hodgkin and Huxley [4], a convenient way to describe the nerve impulse conduction is to think of the nerve fiber as an electrical transmission line. Thus, in its most conventional formulation the Hodgkin-Huxley electrical model assumes currents in extracellular and intracellular fluids to be Ohmic so that the net transmembrane current is the sum of ionic and capacitive currents. The conservation law for current flow across the membrane then reads [3,4]

$$C_m \frac{\partial V}{\partial t} = D \frac{\partial^2 V}{\partial x^2} + I_{\text{ions}}(V). \quad (1)$$

In this formulation, the membrane capacity  $C_m$  is fix while ionic currents  $I_{\text{ions}}$  are functions of the transmembrane volt-

age  $V$  thus providing the feedback necessary to sustain the stimulations of the nerve fiber.

However, while the above electrical-circuit approach puts an emphasis on ionic currents as the direct sources of feedbacks responsible for the self-regulation of the nerve stimulus, there have been several experimental evidences [10,11] of a significant dependence of the membrane capacity on the impulse shape. Namely, in the case of squid giant axons a noticeable change in the membrane capacity at the onset of a nerve impulse has been reported. Moreover, by analyzing the time course of a transmembrane stimulus Cole and Curtis [12] noted that the onset of the abrupt fall in the membrane capacity coincided with a threshold amplitude of the transmembrane excitation. There have been recent attempts (see, e.g., Ref. [11]) to explain all these observations in terms of change in the excitation regime, i.e., a consequence of the nerve impulse moving from the active to the resting phases where the membrane resistivity assumes different values. But this behavior could also be understood as reflecting a self-regulatory function of the membrane vis-a-vis the charges stored in the membrane capacitor, and whose main role is to keep the intensity of the transmembrane excitation within a finite interval.

As we are interested in the electrodynamics of the nerve impulse, it is instructive recalling some of the salient properties of the nerve fiber structure that motivated its classic representation in terms of an electrical cable [12–14], but which also underline the qualitative role of the membrane in the generation of nerve impulse. The nerve fiber is often viewed as a cylinder with walls made from the cell membrane with intracellular and extracellular fluids [9]. In this picture, the intracellular fluid stands for a conductive liquid with a high concentration of potassium ions but low concentration of sodium and chlorine ions, while the cell membrane acts like a barrier preventing ions from the intracellular liquid from mixing with the external solution. The resting potential sets up across the membrane as a result of the difference in ion concentrations. During the resting phase (i.e., nerve polarization), the membrane becomes selectively per-

\*Electronic address: [adikande@ictp.it](mailto:adikande@ictp.it)

meable to ionic currents which flow rapidly into the cell reversing the polarity of the action potential. From the standpoint of the electrical cable representation, the selective and regulatory functions of the nerve membrane suggest a management of ionic charges stored in the membrane capacitance, so the membrane capacitance behaves quite like a capacitive diode (or VARACTOR) in a self-regenerative circuit [15–24] where the capacitance is of a nonlinear capacity with a specific capacity-voltage (CV) characteristic. In general, the specific CV characteristic is needed to maintain desired finite threshold amplitudes of the voltage excitation across the circuit.

The nerve is known to serve as a motor organ for several biological functions, one most important being the neuromuscular activities [2,9] in which the feedback effect of the nerve membrane is reflected through a self-excitability controlling muscular contractions [9]. Therefore a good understanding of the mechanism underlying the generation and propagation of the nerve excitation is relevant for better understanding the functioning of many other organs as well as the biological system as a whole.

The present work aims at probing the consistency of a model for the nerve impulse generation and transmission mechanisms, based on the hypothesis of the membrane as the source of the essential feedback controlling shapes and robustness of the nerve impulse. Our working symbolic circuit is the common nerve transmission line model [9,11], except that we consider the possibility for the membrane capacity to vary with the total amount of ionic charges exchanged across the nerve membrane at some time  $t$ .

In the next section (i.e., Sec. II), after a brief introduction of the model Kirchhoff laws are applied to derive the equations governing the propagation of the transmembrane voltage excitation. These are discrete difference, first-order nonlinear differential equations which can take distinct forms for different CV characteristics of the membrane capacity. In Sec. III, a time series analysis will be carried out to explore the possible shape patterns for the transmembrane excitation that the capacitive feedback is likely to drive. In Sec. IV, the full nerve transmission line equation is discussed in the continuum limit, i.e., when the size of electrical sections of the line is typically very small so that the nerve can be considered infinite. Possibilities for analytical solutions to this equation will be considered for two illustrative CV characteristics that lead to an impulse with both well localized spatial shapes and relatively brief time courses. Sec. V will be devoted to concluding remarks and a brief summary of results.

## II. NERVE TRANSMISSION LINE MODEL AND VOLTAGE EQUATIONS

In excitable biological systems such as the nerve, an action potential propagates in form of wave which can display different shape profiles depending on the response of the main governing biological organ. In this last respect, the nerve impulse can be seen as a potential difference across the plasma membrane of the nerve, and because it is highly selective vis-a-vis the charges exchanged across it the nerve

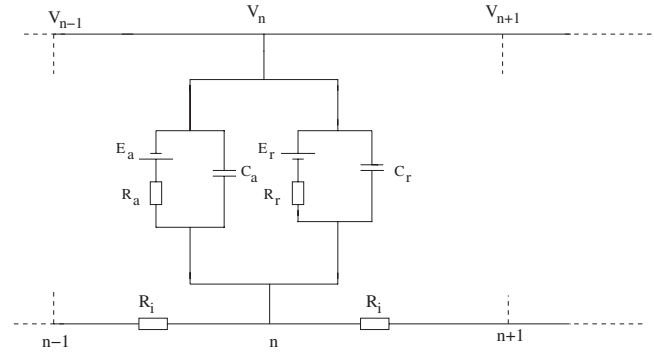


FIG. 1. The symbolic nerve transmission line model under study

membrane (e.g., the axoplasmic layer of the squid giant axon [12–14]) can be considered as a self-regulatory organ in the processes of generation and propagation of the nerve impulse. Electrophysiological evidences suggest that the cell membrane separating the extracellular fluid from the cytoplasm can be represented by a  $RC$  parallel circuit: in this picture the capacity  $C_m$  is related to the charge storage in the lipid membrane, while the resistor  $R_m$  stands for the resistance of ionic channels. In addition, the  $RC$  combination is interspersed with an external resistance  $R_e$  and an internal resistance  $R_i$  representing, respectively, the resistances of the external fluid and the cytoplasm.

We assume that every constant potential change adds linearly to the resting potential and thus can be ignored. Moreover, the radial section of axons suggests an electrical-circuit representation of the nerve transmission equivalent to the long cylindrical electrical cable. Accordingly, characteristic electrical parameters such as  $R_i$ ,  $R_e$ ,  $R_m$  and so on can be readily referred to per unit of the cable length, i.e.,  $r_i = R_i/\Delta x$ ,  $r_e = R_e/\Delta x$ ,  $r_m = R_m/\Delta x$ , where  $\Delta x$  is the size of an elementary circuit.

Instructively, the way biological organs contributing to the nerve impulse are arranged in the nerve fiber is quite relevant in the design of a minimum acceptable theoretical transmission line model. In a myelinated nerve fiber, elementary circuits can be identified through repeated sections of myelin sheets interrupted by nodes of Ranvier. When there is no myelin this arrangement still holds as no nerve component other than the myelin sheet is absent, so that the nerve fiber can be seen as a periodic ladder line with repeated identical circuits. Our working model can therefore be represented by the symbolic transmission line sketched in Fig. 1. It consists of three main parts, namely, the external fluid, the interior of nerve fiber, and the membrane which electrical elements form components of the transmission line [9,11]. To take into account the active and resting states in every excitation cycle, electrical cells of the transmission line will be assumed to group two elementary circuits with similar electrical components but different magnitudes. Denoting by  $E_{a,r}$ ,  $r_{a,r}$ ,  $C_{a,r}$  the membrane electromagnetic field, resistance and capacitance respectively in the active (a) and resting (r) regions, Kirchhoff's laws lead to the following voltage equations, valid in the two elementary circuits composing the  $n^{\text{th}}$  electrical cell (of length  $\Delta x$ ):

$$\frac{\partial Q_{a,r}(V_n)}{\partial t} + \frac{1}{r_{a,r}\Delta x}(V_n - E_{a,r}) = \frac{1}{r_i\Delta x}(V_{n+1} - 2V_n + V_{n-1}), \quad (2)$$

where  $Q_{a,r}(V_n)$  is the total charge available at time  $t$  in the capacitor of the  $a$  or  $r$  section of the  $n^{\text{th}}$  electrical cell, and  $r_i$  is the homogeneous resistance (per unit length of the circuit) of the interior fluid.

Formula (2) refers to a discrete set of partial differential equations which can be solved independently for the voltage passing the active and resting regions of an  $n$  elementary circuit. However, because of continuity requirement in the shape profiles of the voltage in the two regions, appropriate boundary conditions are to be applied. These boundary conditions shall determine the threshold amplitudes and eventually speeds of the voltage excitation in the two regions, in the case when the membrane capacitance has a fixed CV characteristic the continuity condition will not affect the intrinsic profile of the transmembrane impulse as the two equations are similar differing only through magnitudes of their characteristic constant electric elements namely  $E_{a,r}$ ,  $r_{a,r}$  as well as the constant parameters in the CV laws. From what precedes we can concentrate on only one among the two equations in formula (2). Therefore, in all what follows the analysis will be carried out on the following discrete set of differential equations:

$$\frac{\partial Q(V_n)}{\partial t} + \frac{1}{r\Delta x}(V_n - E) = \frac{1}{r_i\Delta x}(V_{n+1} + V_{n-1} - 2V_n). \quad (3)$$

Physically, the left hand side of the last equation represents the sum of the capacitive current across the membrane and the leakage through ion channels, while the right hand side accounts for the propagation of the transmembrane voltage excitation by means of node-to-node transmission. In the present description no phenomenological current is introduced, as we cannot quantalively determine a priori the fractions of the total amount of currents from individuals among the various ions which cross the membrane, without precise information about the responses of the membrane to each ionic species. Instead, we assume that ions reaching the membrane are accumulated in the membrane capacitance which will determine the amount of ionic current crossing the membrane, according to the total voltage set across the capacitance. From this last standpoint, it is ready to view the membrane capacitance as a self-regenerative diode with a well-defined CV characteristic. As already stressed in the introduction, experimental results on the squid giant axons give evidence of an increase in the membrane capacitance in the rising phase of the transmembrane stimulus. So the CV law of the membrane capacitance in this specific context, and probably for many other biological contexts of nerve fibers, can be determined from experimental data. However, our main focus here is the theoretical implication, qualitatively speaking, of the assumption of the nerve membrane capacitor as the main source of feedback governing both shapes and stability of the transmembrane impulse. In this last purpose, we shall consider trial CV characteristics which are polynomial functions of the voltage, two simplest forms implying

the following expressions for the total charge available in the membrane capacitor at any time  $t$ :

$$Q(V) = C_{m0}(1 - \alpha|V|)V, \quad (4)$$

and

$$Q(V) = C_{m0}(1 - \alpha|V|^2)V, \quad (5)$$

where  $C_{m0}$  is the bare value of the membrane capacity and  $\alpha$  in Eqs. (4) and (5) is a parameter having dimension of the inverse voltage and inverse voltage squared, respectively, hereafter referred to as the feedback parameter. Since  $\alpha$  is assumed small in the present study, amplitudes of the transmembrane voltage will always remain within a finite interval with boundary values fixed by the feedback.

### III. TIME SERIES ANALYSIS OF THE TRANSMEMBRANE VOLTAGE EQUATION

The central issue raised by the assumption of the feedback function of the nerve membrane, relates to characteristic features of the impulse profiles governed by this feedback. As we rely on the nonlinear CV characteristics to provide pertinent information on this issue, it is certainly of great instruction questioning currently available experimental data on the issue, in order to retrieve key insights that can guide our analysis. In this last respect, the first relevant aspect concerns the typical shape profile of the propagating nerve impulse which, as the many electrophysiological recordings found in the literature suggest, is pulslike. Second, unlike many other chemical activities occurring in biological systems [25] such as those achieving long-term controls via hormonal mechanisms, the nervous system utilizes ultrafast mechanisms of chemical and electrical transmissions to propagate signals and commands. Brief impulses are thus essential to allow the nervous system mediate short term and even immediate communications, while ensuring control of inter relationships between activities of various body systems. It is therefore interesting to see to which extent the feedback picture of the nerve membrane can account for both the pulse shape and a short time course of the nerve impulse. In this last purpose it is useful to proceed to time series analysis of the voltage Eq. (3), i.e., analyzing its solutions without the spatial spread. Thus, in the absence of the diffusion term we obtain the following single anharmonic oscillator equation:

$$\frac{\partial Q(V)}{\partial t} + \frac{1}{r\Delta x}(V - E) = 0. \quad (6)$$

As the anharmonicity in the last equation stems from the voltage dependence of the membrane capacity, we must expect time variation in the resulting transmembrane excitation to clearly carry signature of the capacitive feedback. We notice about this last point that the case of the nerve fiber with a constant capacity has been discussed at length and solutions are known to be exponentially varying in time with a dominant kink shape. However, because of the linear character of the voltage equation, the kink shape is infinitely extended and in addition has an arbitrary amplitude. For a myelinated fiber, where the myelin sheet strongly screens

current exchanges across the membrane, the membrane resistance is very large so that the voltage equation can be approximated by

$$\frac{\partial Q(V)}{\partial t} = 0. \quad (7)$$

The last equation, for a constant capacity, admits a unique solution which is an arbitrary constant amplitude. As established in Ref. [11], the transmembrane excitation in this specific context is a step impulse with an amplitude unspecified within the linear theory. If now we assume the capacity to vary with the transmembrane voltage as suggested by any one of the two CV laws Eqs. (4) or (5), we find two constant solutions representing two possible distinct thresholds of the transmembrane voltage, one of which is explicitly determined by the capacitive feedback.

Unlike the myelinated fiber just discussed, for which the transmembrane stimulus has a step profile referring to a nerve impulse with a delta shape (spike), the nonmyelinated fiber seems to possess a more rich dynamics as the associate voltage equation, i.e., Eq. (6) suggests. We solved this last equation numerically following a simple fourth-order Runge-Kutta scheme, initial voltages for stable solutions are not unique but should be sufficiently small compared with the threshold values defined by the feedback coefficient  $\alpha$  in the two CV laws Eqs. (4) and (5). Figures 2 and 3 display temporal profiles of the transmembrane voltage (left column) and current (right column) for the two distinct laws of variation in the total membrane charge given by Eqs. (4) and (5), respectively. For all curves characteristic parameters of the model are dimensionless and are given arbitrary values, as our main motivation here is much more a qualitative analysis. Thus, we assumed  $E=50$  and  $C_{m0}r\Delta x=1$  while the feedback parameter  $\alpha$  is varied as follow, from the top pair of graphs to the bottom pair of graphs in the two figures:  $\alpha = 0.0015, 0.002, 0.005, 0.01$ .

The top pair of graphs in the two figures corresponds to temporal profiles of the transmembrane voltage (left) and current (right) for the linear capacity-voltage characteristic Eq. (4), in the case of very small values of the feedback  $\alpha$ . According to the left graph, the voltage increases from a minimum to a maximum threshold with a kink shape that exponentially extends with time. The time course of the transmembrane voltage excitation is thus relatively longer at very small values of the feedback parameter  $\alpha$ , so that the corresponding shapes of transmembrane voltage are still dominated by the exponential behavior predicted within the linear theory [11]. However, as  $\alpha$  increases, profiles of the transmembrane excitation reflect more and more short impulses with well localized shapes. Likewise, on the right graphs the pulse shape of the transmembrane current is more and more well localized when  $\alpha$  is increased, consistently with the reduction in the time course of the voltage excitation observed in the left graphs.

In addition to their sharp profiles, one of the remarkable features of shapes of the transmembrane voltage and current at relatively large values of the feedback parameter  $\alpha$ , is the deviation from a pure exponential variation as it is apparent through the finite tails as  $t$  tends asymptotically to infinity.

This is particularly noticeable in the two last pairs of graphs in Figs. 2 and 3, and reflects their finite time courses due to the anharmonicity from the feedback promoting solitary-wave excitations which are self-reinforcing waves of permanent form.

Though we do not expect none of the two above CV characteristics to give exact description of the physical realm, it would be interesting, nevertheless, to gain insight on the basis of the numerical results obtained in Figs. 2 and 3 onto the most physically relevant form among the two CV characteristics considered. Before getting to that point, it is worth remarking that in the present description the nerve impulse over the nerve transmission line should correspond actually to the potential difference between two boundary nodes of every elementary circuit. Therefore, since the membrane resistance is constant the nerve impulse and transmembrane current must change similarly with time over one elementary circuit of the nerve transmission line. With this consideration in mind, we compared time variations of the transmembrane currents in Figs. 2 and 3 for same values of the feedback  $\alpha$ . On Fig. 3 the pulse shape of the transmembrane current is clearly apparent at positive times for sufficiently large values of the feedback, and is expected to be more and more pronounced as  $\alpha$  increases in contrast to Fig. 2 where there is no pulse profile emerging. Remarkably, the pulse profile in Fig. 3 with a relatively longer branch of decreasing excitation toward the resting phase compared with the rising phase is in qualitative agreement with the typical profile reported in most electrophysiological recordings. However, as already said, we can only gain a qualitative understanding from the two CV characteristics assumed in this study, a more elaborate formulation is required using exact expression(s) of the CV characteristic which can be extracted from experimental data for each specific nerve organ.

#### IV. PHYSICAL VIRTUES OF THE CONTINUUM NONLINEAR NERVE TRANSMISSION LINE EQUATION

In the previous section, time series of the voltage Eq. (3) have clearly revealed a strong influence of the capacitive feedback of the nerve membrane on the transmembrane voltage excitations. Namely, we found that the capacitive feedback drives well-localized short pulses which are relatively more stable than the exponentially extended objects found in the linear regime [11]. Here we shall discuss the physics behind the full nerve transmission line Eq. (3) with a specific emphasis on the effect of the capacitive feedback on the transmission properties of the nerve impulse. Assuming the length of elementary sections of the line to be very small so that the line can be considered infinite, the continuum limit approximation in the weak dispersion regime leads from the discrete Eq. (3) to the following one:

$$\frac{\partial Q(V)}{\partial t} + \frac{1}{r\Delta x}(V - E) = \frac{\Delta x}{r_i} \frac{\partial^2 V}{\partial x^2}. \quad (8)$$

This is a continuum equation which, for a constant capacitance, reduces to a linear dissipative partial differential equation admitting exact analytical solutions [11]. For this last

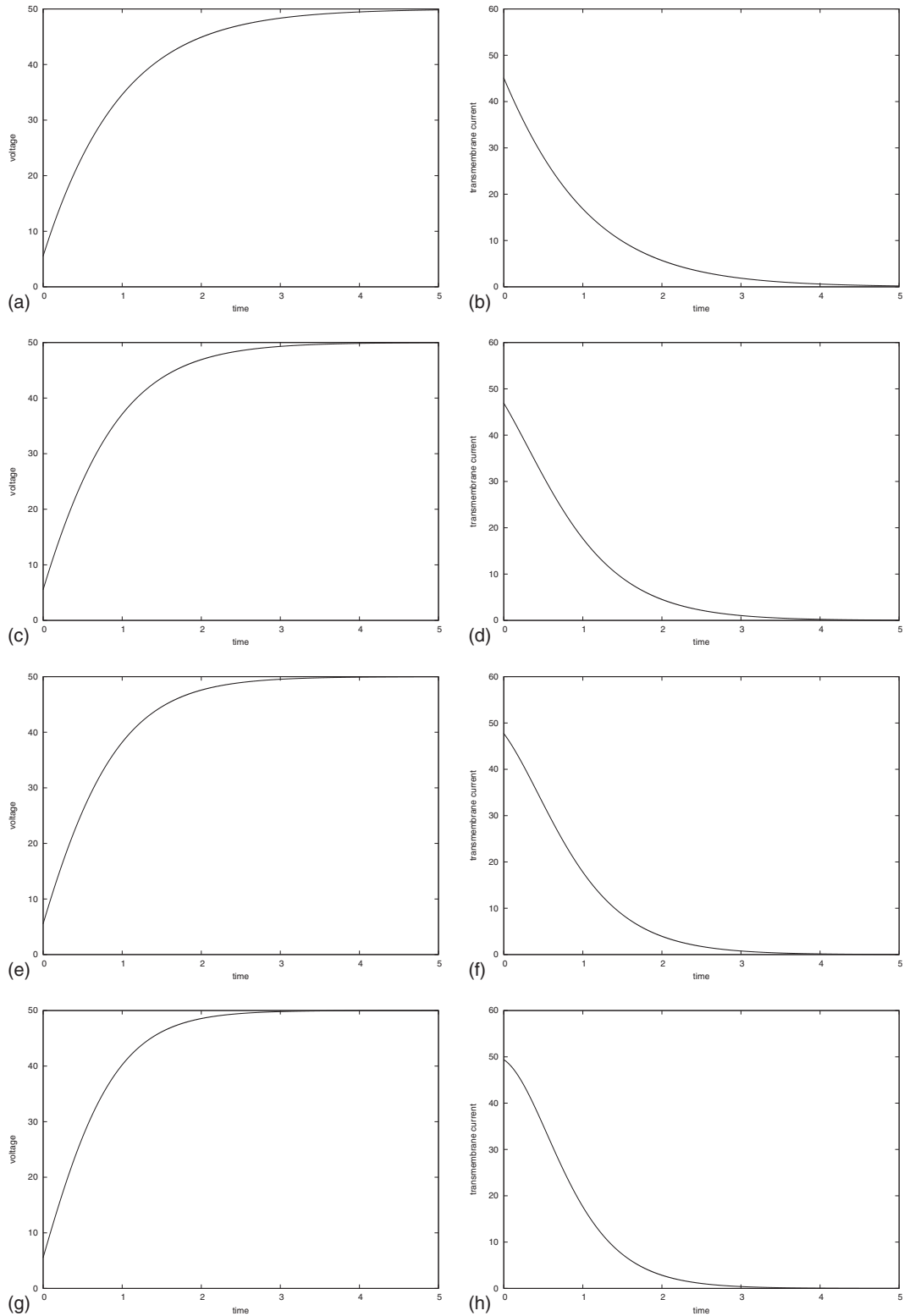


FIG. 2. Time courses of the transmembrane voltage (left column) and current (right column), from numerical simulations of the voltage Eq. (6) with the charge-voltage characteristic Eq. (4). For all curves  $E=50$  and  $C_{m0}r\Delta x=1$ , while  $\alpha$  is increased from the top to the bottom pairs of graphs as follows:  $\alpha=0.0015, 0.002, 0.005, 0.01$ .

case, it has been found that the nerve impulse has a kink shape as it propagates across the nerve fiber. However, because of the linear character of the transmission line, the excitation experiences spatial spreading as a result of the

whole set of associate spatial parameters (i.e., characteristic lengths and threshold voltages) depending on the propagation velocity. Thus, depending on the magnitudes of spatial parameters and the transmission speed, the dispersion rela-

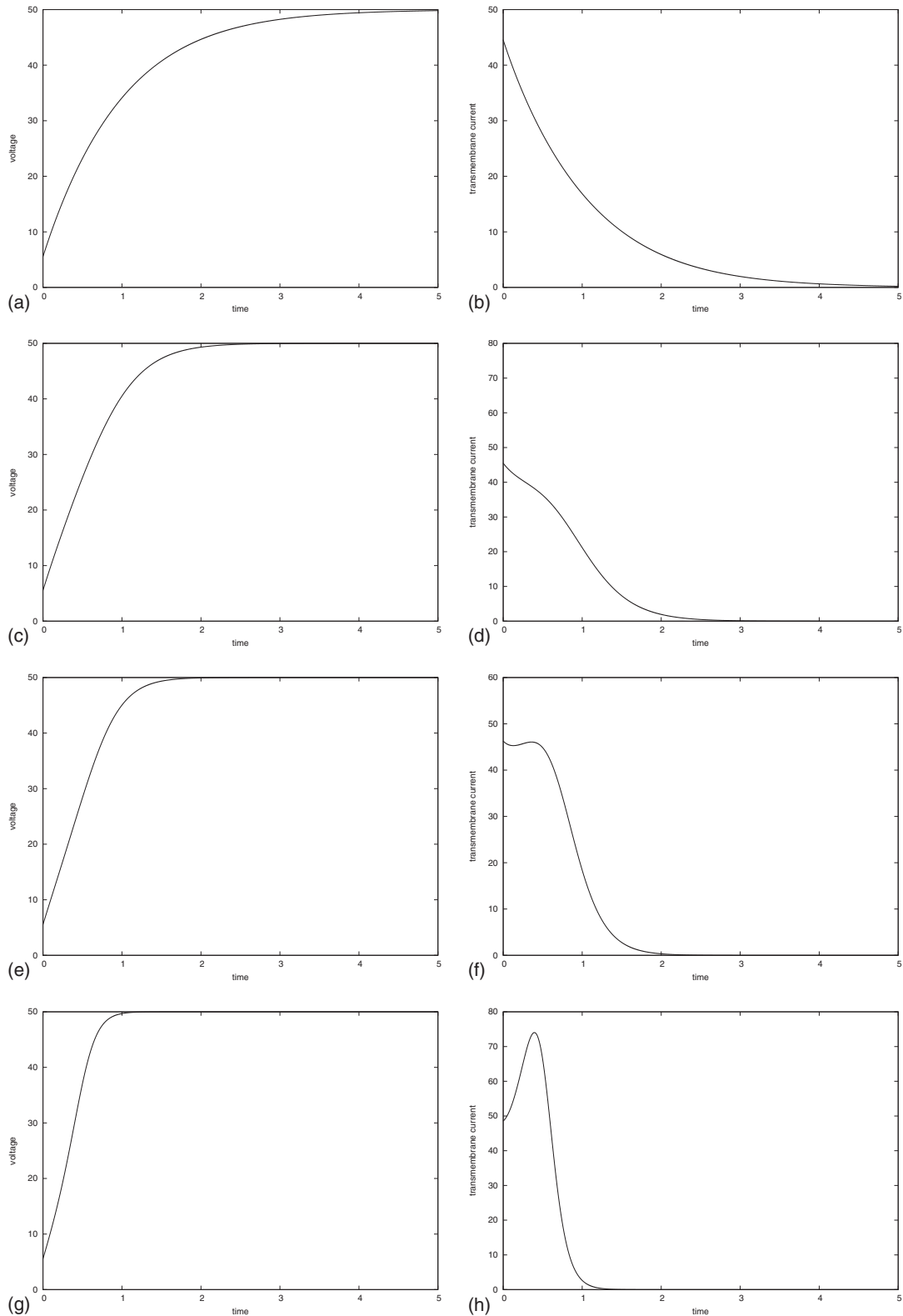


FIG. 3. Time courses of the transmembrane voltage (left column) and current (right column), from numerical simulations of the voltage Eq. (6) with the charge-voltage characteristic Eq. (5). Parameter values are the same as in Fig. 2.

tion gives rise either to a pure exponential amplification/decay of the transmembrane excitation, or an exponential amplification/decay with a sinusoidal modulation in both space and time. When the capacitive feedback of the nerve

membrane is taken into consideration, the voltage Eq. (8) turns to a nonlinear partial differential equation with a linear dissipation. Although this equation seems difficult to solve analytically, solutions at finite nonzero values of the feed-

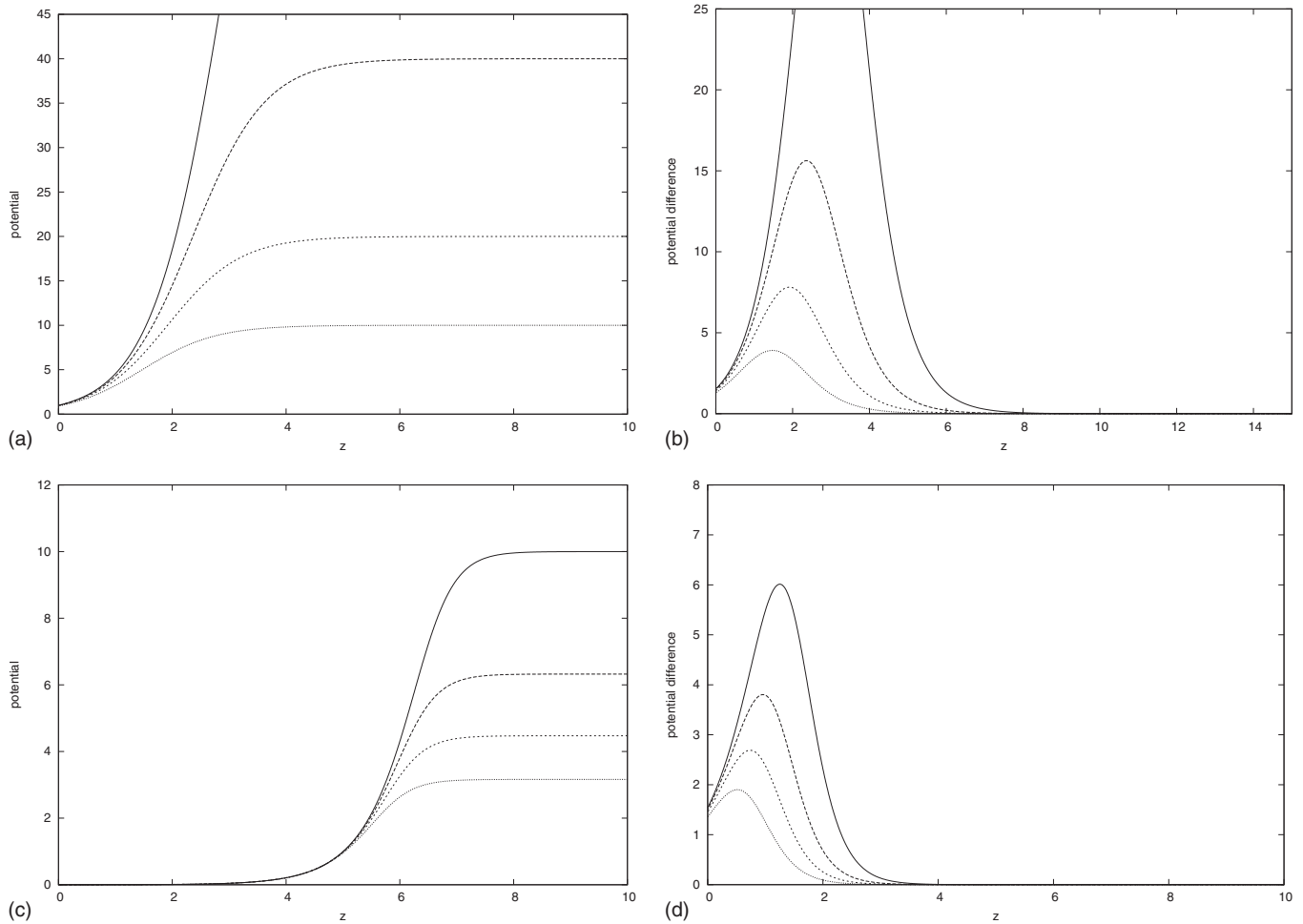


FIG. 4. Shapes of the transmembrane voltage (left graphs) and current (right graphs), corresponding to the charge-voltage characteristic Eq. (4) (top pair of graphs) and Eq. (5) (bottom pair of graphs), for different values of the feedback parameter  $\alpha$  as given in the text.

back  $\alpha$  are expected not to differ from Figs. 2 and 3 by virtue of the Galilean transformation and translational invariance in a reference frame attached to the wavefront of the propagating excitation. Ultimately we can expect an impulse with a sharp spatial and short duration profile and in turn, a robust excitation against the line dispersion consequent upon the compensation of the line dispersion by the anharmonicity provided by the capacitive feedback.

It has been established [11] that for myelinated fibers with constant capacity, the exact solution to the continuum Eq. (8) is given in terms of the error function. Hence, in this specific physiological context the nerve impulse is Gaussian with a characteristic width and intensity which are directly and inversely proportional, respectively, to the impulse propagation time. Examining solutions to the nerve fiber Eq. (8) in the same physiological condition but now with the capacitive feedback, we find the analytical solution:

$$V(x,t) = \left[ \alpha + \exp \frac{x + \vartheta t}{\ell(\vartheta)} \right]^{-1}, \quad (9)$$

for the linear CV law Eq. (4) and

$$V(x,t) = \left[ \alpha + \exp -2 \frac{x + \vartheta t}{\ell(\vartheta)} \right]^{-1/2} \quad (10)$$

for the quadratic CV law in Eq. (5). In Eq. (9) and (10) the quantity  $\ell(\vartheta)$  is defined as

$$\ell(\vartheta) = \frac{\Delta x}{r_i C_{m0} \vartheta}, \quad (11)$$

and stands, in the first solution Eq. (9), for the characteristic width of the transmembrane voltage excitation while for Eq. (10) it corresponds to half the impulse characteristic width. On Fig. 4, we plot the voltage excitation suggested by the two solutions (left graphs) as well as the corresponding currents (right graphs), for arbitrary values of the constant (and dimensionless) parameters in the propagation equation but different arbitrary values of the feedback  $\alpha$ , i.e., 0.01, 0.025, 0.05, 0.1.

In each of the four graphs, when  $\alpha$  increases from 0.01 to 0.1 the transmembrane voltage and current are more and more well localized excitations in the space-time coordinate  $z$ . As expected, the sharpest structures emerge for the quadratic CV characteristic which, according to graphs of Fig. 3, gives rise to impulses with the shortest durations.

## V. CONCLUSION

In this study, we addressed the problem of the nerve impulse generation and transmission in a cable model where the nerve membrane is assumed to provide the essential feedback for stabilizing the impulse. In this context, the nerve capacitance was represented by a self-regenerative diode with a nonlinear charge-voltage (QV) characteristic. By considering two different elementary QV laws for theoretical illustration, time series of the transmembrane voltage and current have revealed a rich family of shape patterns characterized by well-localized short impulse profiles at relatively strong feedback.

Although the quadratic CV characteristic apparently best represents the nerve impulse shape among the two laws considered in our study, this certainly does not mean that it constitutes the ideal representation of the feedback function of the membrane capacitance as expected *in vivo*. In fact, the assumption of very small values of the feedback parameter  $\alpha$  is suggestive of a truncated expression from some more complex function within a polynomial expansion in the weak  $\alpha$  regime. From this last standpoint, several forms of such

functions can be envisaged two most common in nonlinear electronics being the logarithmic and power-laws [15–18,21,22,26] characteristics. However, obtaining a precise form of the CV characteristic actually requires an analysis of reliable experimental data on the nerve impulse transmission in defined physiological conditions. A deeper study involving available experimental data on the response of the nerve membrane capacitance to the transmembrane excitations is therefore necessary to gain complete qualitative as well as quantitative understandings of the nerve impulse generation and transmission, within the framework of the proposed approach based on the picture of a nerve stimulus driven by the feedback of the membrane capacitance.

## ACKNOWLEDGMENTS

The authors thank the referee for pertinent suggestions that greatly contributed to improve the original manuscript. A.M.D. is indebted to the Max Planck Institute for the Physics of Complex Systems (MPIPKS) Dresden, Germany for permitting a visit during which part of simulations in the work was carried out.

- 
- [1] F. Rattay, *Electrical Nerve Stimulation: Theory, Experiments and Applications* (Springer, Vienna, 1990).
- [2] R. D. Keynes and D. J. Aidley, *Nerve and Muscle*, 3rd ed. (Cambridge University Press, Cambridge, 2001).
- [3] A. L. Hodgkin and A. F. Huxley, *J. Physiol.* **104**, 176 (1945).
- [4] A. L. Hodgkin and A. F. Huxley, *J. Physiol.* **177**, 500 (1952).
- [5] E. N. Warman, W. M. Grill, and D. Durand, *IEEE Trans. Bio-Med. Electron.* **39**, 1244 (1992).
- [6] W. M. Grill, *IEEE Trans. Bio-Med. Electron.* **46**, 918 (1999).
- [7] O. V. Aslanidi and O. A. Mornev, *JETP Lett.* **65**, 579 (1997).
- [8] A. G. Richardson, C. C. McIntyre, and W. M. Grill, *Med. Biol. Eng. Comput.* **38**, 438 (2000).
- [9] W. Peasgood, L. A. Dissado, C. K. Lam, A. Armstrong, and W. Wood, *J. Phys. D* **36**, 311 (2003).
- [10] S. Takashima, *Biophys. J.* **26**, 133 (1979).
- [11] I. Tasaki and G. Matsumoto, *Bull. Math. Biol.* **64**, 1069 (2002).
- [12] K. S. Cole and H. J. Curtis, *J. Gen. Physiol.* **22**, 649 (1939).
- [13] J. Metzuzals, I. Sasaki, S. Terakawa, and D. F. Clapin, *Cell Tissue Res.* **221**, 1 (1981).
- [14] K. S. Cole and A. L. Hodgkin, *J. Gen. Physiol.* **22**, 671 (1939).
- [15] M. Toda, *J. Phys. Soc. Jpn.* **23**, 501 (1967).
- [16] R. Hirota and K. Suzuki, *J. Phys. Soc. Jpn.* **28**, 1366 (1970).
- [17] R. Hirota and K. Suzuki, *Proc. IEEE* **61**, 1483 (1973).
- [18] T. Yoshinaga and T. Kakutani, *J. Phys. Soc. Jpn.* **56**, 3447 (1987).
- [19] B. Z. Essimbi, Alain M. Dikandé, T. C. Kofané, and A. A. Zibi, *J. Phys. Soc. Jpn.* **64**, 2361 (1995).
- [20] B. Z. Essimbi, Alain M. Dikandé, T. C. Kofané, and A. A. Zibi, *Phys. Scr.* **52**, 17 (1995).
- [21] H. C. Hsieh, *J. Appl. Phys.* **62**, 2095 (1987).
- [22] H. Shi, C. W. Domier, and C. Luhmann, *J. Appl. Phys.* **78**, 2558 (1995).
- [23] F. Martin and X. Oriols, *J. Appl. Phys.* **78**, 2802 (2001).
- [24] K. Tse Ve Koon, J. Leon, P. Marquié, and P. Tchofo-Dinda, *Phys. Rev. E* **75**, 066604 (2007).
- [25] Compared with the cycle of electrochemical processes occurring in the nervous system, the time scale for chemical reactions in the endocrine system for instance, is typically far larger.
- [26] H. Nagashima and Y. Amagishi, *J. Phys. Soc. Jpn.* **45**, 680 (1978).